Proceedings of 2004 IEEE/RSJ International Conference on
Intelligent Robots and Systems
September 28 - October 2, 2004, Sendai, Japan

Grip Force Control for an Elastic Finger using Vision-based Incipient Slip Feedback

Atsutoshi Ikeda, Yuichi Kurita, Jun Ueda, Yoshio Matsumoto, Tsukasa Ogasawara
Graduate School of Information Science,
Nara Institute of Science and Technology (NAIST), Nara, 630-0192, Japan.

Abstract— **In this paper, a grip-force control of an elastic object is proposed based on a visual slip margin feedback. When an elastic object is pressed and slid slightly on a rigid plate, a partial slip, called "incipient slip" occurs on the contact surface. The slip margin between an elastic object and a rigid plate is estimated based on the analytic solution of Hertzian contact model. A 1 DOF gripper consists of a camera and a force sensor is developed. The slip margin can be estimated from the tangential force measured by a force sensor, the deformation of the elastic object and the radius on the contact area both measured by a camera. In the proposed method, the friction coefficient is not explicitly needed. The grip force is controlled by a direct feedback of the estimated slip margin, whose stability is analytically guaranteed. As a result, the slip margin is maintained to a desired value without occurring the gross slip against a disturbance load force to the object.**

Keywords— **Grip Force Control, Elastic Object, Hertzian Contact, Incipient Slip, Visual Feedback.**

I. Introduction

It is considered that the dexterity in human's grasping and manipulation is due to the tactile sensation of the fingertips. As a result, human successfully controls the grip force on an object whose friction coefficient is not obvious. When a fingertip is pressed and slid on a rigid plate, the deformation of the fingertip can be assumed as that of an elastic object. The incipient slip is known as a partial slip of the contact area between the elastic object and the rigid plate. Johansson *et al.* have shown that perceiving this incipient slip takes an important role in human grasping motion[1].

For the purpose of achieving robotic grasping inspired from human tactile sensation, a number of tactile sensors have been developed[2][3][4][5]. Compared to the development of tactile sensors, there are not many researches on the grip-force control based on incipient slip sensing using these sensors. Melchiorri proposed a grip-force control based on the combination of a force/torque sensor and pressure distribution sensor[6]. However, the friction coefficient between the fingertip and the object should be known beforehand the control. Maeno *et al.* proposed a method of grip-force control based on the measurement of the internal strain distribution in the contact between a fingertip and a rigid plate aiming at the case where the friction coefficient is unknown[7]. However, it is difficult to increase the spatial resolution because many strain gauges should be located inside the sensor. Moreover, the contact stability by a direct feedback of the incipient slip sensing has not been shown.

In this paper, a method of slip margin estimation and a vision-based grip force control are presented during the incipient slip. The slip margin is calculated from *Hertzian contact model*[8] of an elastic object by measuring the tangential force, the radius of the contact area and the displacement of elastic object. In order to estimate the deformation of the object, the eccentricity[9] is applied. A 1 DOF gripper with a force sensor and a camera for measuring the contact area is developed. The grip force is controlled using a direct feedback of the slip margin without knowing the friction coefficient. The proof of the contact stability by the proposed grip control is analytically obtained. As a result, the slip margin is maintained to a desired value without occurring the gross slip against a disturbance force to the object.

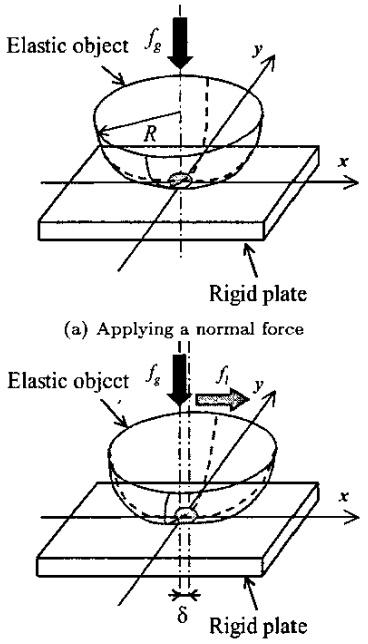

(a) Applying a normal force

(b) Applying a normal and tangential force

Fig. 1. Contact model of an elastic object and a rigid plate

II. Grip-force Control based on Incipient Slip Measurement

A. Contact between an Elastic Object and a Rigid Plate

The contact between an elastic sphere and a rigid plate is called *Hertzian contact*[8] and various analysis have been

0-7803-8463-6/04/$20.00 ©2004 IEEE

presented [10]. Fig. 1 shows the schematic diagram of the contact when applying the normal force f_g and the tangential force f_l. In this analysis, we consider the situation where the contact holds, therefore $f_g > 0$. Considering the sphere is symmetry around the direction of f_g, we can assume that f_l denotes the absolute value of the tangential force without losing the generality, i.e., $f_l > 0$.

When the elastic sphere is pressed and slid on a rigid plate, the sphere deforms depending on f_g and f_l. The radius of the contact area a is derived from the following equation:

$$a = \left(\frac{3f_gR}{2E'}\right)^{1/3} \tag{1}$$

where R is the radius of the elastic object and $E' = 2(E_1/(1-\nu_1^2)+E_2/(1-\nu_2^2))$ is the equivalent stiffness coefficient. Young's modulus and Poisson of the elastic object and the rigid plate are E_1, ν_1 and E_2, ν_2, respectively.

The distribution of the normal pressure $P(f_g, r)$ in the contact area and the maximum normal pressure $P_{max}(f_g)$ are derived from the following equation[8]:

$$P(f_g, r) = \frac{3f_g}{2\pi a^2}\left(1 - \frac{r^2}{a^2}\right)^{1/2} \tag{2}$$

where $r = \sqrt{x^2+y^2}$ and $[x, y]$ is the position based on the contact center. The maximum normal pressure is given by: $P_{max} = 3f_g/(2\pi a^2)$. The normal force around the boundary is smaller than the normal force around the center. Therefore a slip between the elastic object and the rigid plate occurs from the boundary region.

When the whole contact surface slips, the elastic object begins to slip completely to the rigid plate, which is called the "gross slip". The partial slip that occurs before the gross slip is called the "incipient slip"[1]. In this paper, the contact region where a partial slip occurs is called as the slip region. The contact region where the objects surface is stuck is called as the stick region. The distance c from the contact center to the boundary between the stick region and the slip region is derived by:

$$c = a(1-\Phi)^{1/3} \tag{3}$$

where $\Phi \triangleq f_l/\mu f_g$ is the tangential force coefficient. μ is the friction coefficient of the contact area. The distribution of the tangential pressure $T(f_g, r)$ in the slip region and the stick region are derived as follows:

$$T(f_g, r) = \begin{cases} \mu P_{max}\left(1 - \frac{r^2}{a^2}\right)^{1/2} \\ \qquad (\text{Slip region} : c < r \le a) \\ \mu P_{max}\left(1 - \frac{r^2}{a^2}\right)^{1/2}\left(1 - \frac{c}{a}\right) \\ \qquad (\text{Stick region} : 0 < r \le c) \end{cases} \tag{4}$$

The tangential pressure becomes maximum on the boundary between the stick region and the slip region. Suppose the elastic object deforms by applying f_g and f_l. A relative displacement δ shown in Fig. 1(b) is occurred by the deformation of the elastic object. The analytic solution has already been obtained as follows[10]:

$$\delta = \frac{3\mu f_g}{16a}\left(\frac{2-\nu}{G}\right)\left\{1 - \left(1 - \Phi^{2/3}\right)\right\} \tag{5}$$

where $G = E/\{2(1+\nu)\}$.

Recently, Xydas *et al.* presented that the radius of contact is proportional to the normal force raised to the power of from 0 to 1/3[11]. In this sense, the Hertzian contact model shown in (1) is only a part of this model. However, this model has not been expanded to the case where the normal and the tangential force are simultaneously applied. In this paper, an analytic solution of the deformation of the elastic object is required for this case. Therefore, the analytic result based on the *classic* Hertzian model shown in (5) is applied.

B. Slip Margin

In order to keep the contact without occurring a slip, the normal force f_g corresponding to the load force f_l should be determined so as to satisfy the friction condition given by the friction cone. The slip margin $\gamma (0 \le \gamma \le 1)$ is used as an index of this contact stability:

$$\gamma = 1 - \Phi \tag{6}$$

When the contact area is completely stuck, $\gamma = 1$ holds. The incipient slip occurs as γ decreases and the elastic object completely slips when $\gamma = 0$. As shown in (6), the slip margin γ is easily obtained if Φ is given. It can be said that the estimation of Φ is almost equivalent to the estimation of γ. Hereafter, we use "slip margin" to Φ unless it causes a confusion.

C. Vision-based Control of Grip force

Fig. 2 shows the result of a preliminary experiment. The contact area is measured by a camera through a transparent plate. A feature point(dot) is drawn on the apex of an elastic sphere. In the figure, the blight area presents the contact area, and the feature point is shown by the intersection of two orthogonal lines. When the load force is increased, the object begins to slip from the boundary of the contact area and the slip region expands toward the center. Therefore, the relative position of the feature point, which is in the stick region in the contact area, changes whose displacement is given by (5).

As described above, there exist slip region and stick region in the contact area. The diameter of the stick region becomes small according to (3) by increasing the load force; however, this change of the stick region can not be directly observed by a camera.

The basic concept of this paper is to estimate the slip margin, i.e., the change of the stick region, based on the displacement of the feature point. The estimated slip margin is used to calculate the grip force. By estimating the

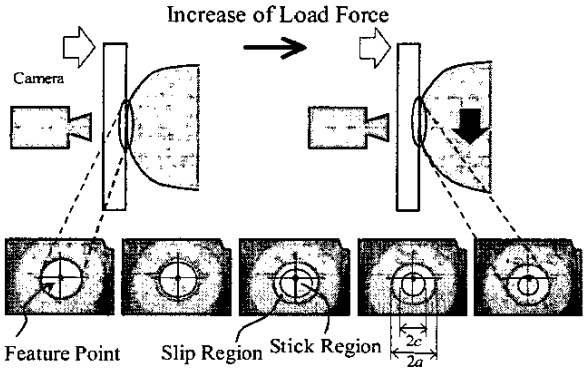

Fig. 2. Deformation of the Contact Area

margin during the incipient slip, a stable grasping is realized against the change of the load, e.g., disturbance force.

III. Estimation of Slip Margin from Deformation of the Contact Area

In this section, a method of estimating Φ is presented by applying (5). In (5), G and ν are known material constants of the elastic object. Then, δ, μ, f_g, and a are needed to estimate Φ by inverse solution of (5). As will be shown in the following sections, we use a camera to measure the contact surface, then δ and a are measured from this image. Additionally, f_g is obvious since it is the output of the actuator itself. The remaining unknown variable is the friction coefficient μ; however we focus on the grip-force control without knowing μ, therefore the following transformation of (5) is applied dividing both sides by f_l.

$$\frac{\delta}{f_l} = \frac{3}{16a}\frac{1}{\Phi}\left(\frac{2-\nu}{G}\right)\left\{1-\left(1-\Phi^{2/3}\right)\right\} \quad (7)$$

The following equation is obtained by collecting Φ:

$$\alpha^3\Phi^2 + (1-3\alpha^2)\Phi + (3\alpha - 2) = 0 \quad (8)$$

where $\alpha = 16Ga\delta/(6-3\nu)f_l$. The solution of (8) Φ_a and Φ_b are obtained as follows:

$$\Phi_a = \frac{-(1-3\alpha^2) - \{(1-3\alpha^2)^2 - 4\alpha^3(3\alpha-2)\}^{1/2}}{2\alpha^3} \quad (9)$$

$$\Phi_b = \frac{-(1-3\alpha^2) + \{(1-3\alpha^2)^2 - 4\alpha^3(3\alpha-2)\}^{1/2}}{2\alpha^3} \quad (10)$$

Φ_a corresponds to Φ in the incipient slip condition In contrast, Φ_b corresponds to Φ in the gross slip condition.

Based on these analyses, Φ_a in the incipient slip condition can be calculated from (9) by measuring δ, f_l, and a. By using this estimated Φ_a, a grip-force control during the incipient slip can be applied, i.e., it is unnecessary to estimate μ by slipping the object once in the gross slip condition. Hereafter, we use Φ in the same meaning of Φ_a.

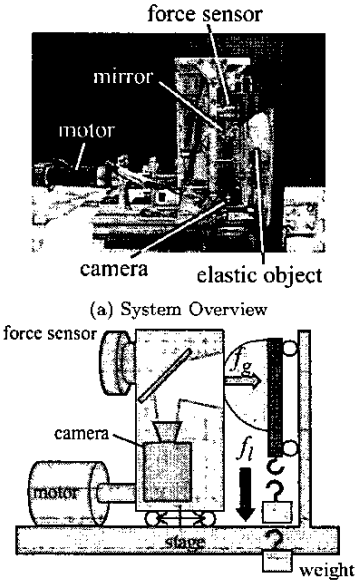

(a) System Overview

(b) Prime Components of the System

Fig. 3. Experimental System

IV. High-accuracy Estimation of the Slip Margin

A. Robotic Gripper with Contact Area Measuring Device

A 1 DOF(degree of freedom) robotic gripper was developed as shown in Fig. 3. Fig. 3(a) shows the overview of the experimental system, and Fig. 3(b) shows the components.

A measuring device including a camera and a 6-axis force sensor[12] is used to measure the contact area between the elastic object and the rigid plate. A small CCD camera(Keyence: CK-200), a $\pi/4$ [rad] angled mirror, and high brightness LED are installed in the device to observe the contact area. The camera captures the image of 320×240[pixel] in about 30[fps] through the transparent rigid plate made from acrylic. Force and torque on the contact area are measured by a 6-axis force/torque sensor(BL-Autotec: Nano 4/5-s15).

These sensors are installed in the aluminum frame fixed on a 1DOF slider. The slider is driven by a geared motor with encoder(Maxon: DC motor). The desired torque of the motor is realized by current control. The elastic object with a semispherical form of radius 20[mm] is used. The elastic object is made from gel(Exseal Co. Ltd.) which is specially designed to have material characteristics of human's skin shown in Table I. The elastic object is attached on a plate and a load force is applied to the elastic object by suspending a weight.

A feature point is drawn on the apex of the elastic object. Fig. 4(a) shows the captured image of the contact area by the constructed device. The captured image is converted to gray scale image and smoothed by 5×5 median filter. Fig.

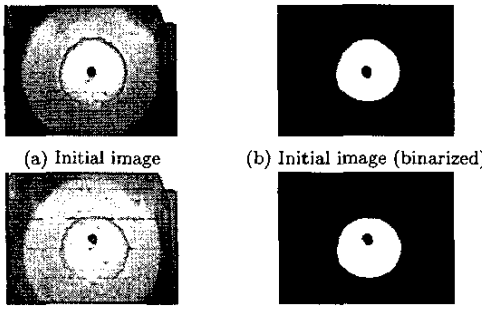

(a) Initial image (b) Initial image (binarized)

(c) Applying load force (d) Applying load force (binarized)

Fig. 4. Image of contact area

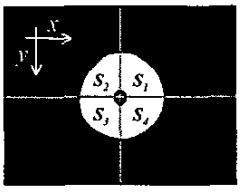

Fig. 5. Separation of the contact area

4(b) shows the binarized image with a certain threshold. Fig. 4(c) and (d) show the contact area when a downward load force is added to the elastic object. When the load force is applied, the contact area is deformed depending on the direction and the magnitude of the load force. Therefore, the relative position of the feature point changes in the contact area. As shown in the figures, the deformation can be observed by this image processing.

B. Eccentricity

In order to calculate Φ, the load force f_l, the displacement δ, and the radius a are necessary. The sensing resolution of δ directly measured from the captured image is not high because δ is very small in comparison with the resolution of the captured image. In this paper, the "eccentricity"[9] is used as an index of the deformation of the elastic object. As a result, a high-accurate estimation of the slip margin is realized.

Fig. 5 shows the image where the contact area is separated into four parts based on the feature point. Each part is numbered in counterclockwise. The whole contact area S, the deformation of the contact area along x-axis S_x and the deformation of the contact area along y-axis S_y are calculated as follows:

TABLE I
MATERIAL CONSTANT OF ELASTIC OBJECT

radius	R	0.02[m]
Young's modulus	E	50000 [N/m^2]
Poisson	ν	0.48

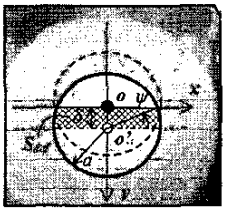

Fig. 6. Eccentricity geometrical model

$$S = S_1 + S_2 + S_3 + S_4 \quad (11)$$

$$S_x = (S_1 + S_4) - (S_2 + S_3) \quad (12)$$

$$S_y = (S_3 + S_4) - (S_1 + S_2) \quad (13)$$

where S_1, S_2, S_3 and S_4 are the area of each part. The image at the neutral position is registered as a template. From the template image, the contact area S_s, the deformation of the contact area along x-axis S_{sx} and the deformation of the contact area along y-axis S_{sy} are calculated from (11), (12), and (13). S_t, S_{tx} and S_{ty} of the target image after applying a load force are also calculated. Finally, the eccentricity e_x, e_y are defined as follows:

$$e_x \triangleq \frac{S_{tx}}{S_t} - \frac{S_{sx}}{S_s} \quad (14)$$

$$e_y \triangleq \frac{S_{ty}}{S_t} - \frac{S_{sy}}{S_s} \quad (15)$$

The eccentricity is a dimensionless value normalized by contact area.

C. Physical Meaning of the Eccentricity

The physical meaning of the eccentricity is examined from the analysis on the elastic deformation. Suppose a case where the contact area is displaced at the length of δ from the neutral position as shown in Fig. 6. To simplify the discussion, the contact area is assumed as a circle, and the direction of the load force is along y-axis. In the figure, o denotes the feature point drawn on the elastic object and o' denotes the center of the contact area. The hatched area S_{def} of the contact surface is calculated by:

$$S_{def} = \delta a \cos\psi + a^2\psi \quad (16)$$

where a is the radius of the contact area, δ is the distance between the center of the contact area and the center of the feature point, ψ is the angle made by the x-axis and the radius from o' to the edge of S_{def}. Assume $S_{sx} = 0$ at the neutral position. Recall $\sin\psi = \delta/a$. The eccentricity along x-axis is obtained by substituting (16) into (15) as follows:

$$e_y \triangleq \frac{S_{ty}}{S_t} - \frac{S_{sy}}{S_s} = \frac{2S_{def}}{\pi a^2}$$

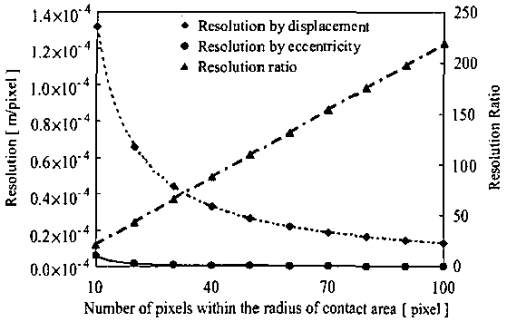

Fig. 7. Comparison of Resolution

$$= \frac{2}{\pi}(\psi + \cos\psi \sin\psi) \tag{17}$$

When the deformation of the elastic object is small where $\delta/a \ll 1$, we can assume that $\psi \simeq \sin\psi$, $\cos\psi \simeq 1$. Finally, the following linear approximation is obtained.

$$e_y \simeq \frac{4\delta}{\pi a} \tag{18}$$

This indicates that the eccentricity is approximately linear to the displacement δ. In order to solve (8) using the eccentricity instead of δ, α is calculated as follows:

$$\alpha = \frac{4\pi G a^2 \sqrt{e_x^2 + e_y^2}}{(6-3\nu) f_l} \tag{19}$$

D. Improvement of Measurement Accuracy

Φ can be estimated in high-resolution by using e_x or e_y rather than δ that is directly measured from the captured image. Fig. 7 shows the spatial resolution of the deformation of the elastic object. In this figure, the method using e_x, e_y and the one directly measuring δ are compared. In this calculation, the radius of the contact area is set constant and the displacement is set as $\delta = 0.67a$. The horizontal axis denotes the number of pixels a_m within the radius a of the contact area. The vertical axis shows the actual length given one pixel, i.e., quantization error. The solid line shows the resolution of the deformation that is directly calculated from the displacement δ. The broken line shows the resolution of the deformation that is calculated from the eccentricity. The dashed line shows the ratio of the resolution dividing the resolution of eccentricity by one of direct measurement.

When the eccentricity is used, the resolution of the deformation of the elastic object is from 50 to 100 times higher in comparison with δ within the range($40 \leq a_m \leq 60$) of the contact radius. The reason of this difference is considered as follows; in the direct measurement of δ, the number of the pixels between the contact center and the feature point is merely counted. In contrast, the displacement is measured by 2 dimensional way in the calculation of the eccentricity, resulting in high accuracy. In addition, the resolution increases as the resolution of the camera increases; however this tendency is stronger in the case using the eccentricity.

V. Grip Force Control based on Slip Margin Feedback

A. Stability of Grip Force Control

In this research, the grip force is controlled by a direct and linear feedback of the slip margin:

$$\dot{f}_g = k(\gamma_d - \gamma(t)) = k(\Phi(t) - \Phi_d) \tag{20}$$

where $k(>0)$ is a feedback gain and $\gamma_d = 1 - \Phi_d$ is the target slip margin. The applying force f_g is updated by the differential of the slip margin. The advantage of this control law is that the calculation is easy and μ is not explicitly needed.

The following equation is derived by substituting $\Phi = f_l/\mu f_g$ and $\Phi_d = f_l/\mu f_{gd}$ into (20).

$$\dot{f}_g = k f_l \frac{f_{gd} - f_g}{\mu f_g f_{gd}} \tag{21}$$

where f_{gd} is the desired force which realizes Φ_d. Note the magnitude of f_{gd} is unknown. Let $\varepsilon = f_{gd} - f_g$ be the error of the force, then (21) is transformed as follows:

$$\dot{\varepsilon} = -p_1 \frac{\varepsilon}{p_2 - \varepsilon} \tag{22}$$

where $p_1 = k f_l/(\mu f_{gd})(>0)$ and $p_2 = f_{gd}$. The solution of (22) is obtained as follows:

$$\varepsilon(t) = -p_2 w\left(-\frac{e^{-\frac{p_1 t + C}{p_2}}}{p_2}\right) \tag{23}$$

where $w(z)$ is Lambert's W function that satisfies $z = we^w$ [13]. In the W function, $w \to 0$ holds when $z \to 0$. Therefore $\varepsilon \to 0$ holds where $t \to \infty$, since $-e^{-(p_1 t + C/p_2)}/p_2 \to 0$. As a result, the stability of the proposed force control is guaranteed for any Φ_d. Note that the presented analysis does not depend on how to estimate Φ.

Although the details of the control scheme of human grasping has not been cleared, a direct feedback of the slip margin can be considered as one possible solution; human senses the slip margin through the change of the stick region. Equation (3) shows its close relation between the slip margin and the size of the stick region. Therefore we use (20) and show its stability and validity for grip control.

B. Experiment

The experiment of grasping the elastic object is performed by using the constructed device. A discrete type of control law of the grip force is obtained as follows:

$$f_{g(t)} = f_{g(t-T)} + k_d(\Phi_d - \Phi(t)) \quad (24)$$

where T is the sampling time of the camera about $T = 40$[msec] and the feedback gain is set $k_d = 0.3$. The desired value is set $\Phi_d = 0.2(\gamma_d = 0.8)$.

A load force of 1.37[N] is applied at the time of $t = 23.0$[sec], then it is increased to 2.74[N] at $t = 57.0$[sec]. Fig. 8(a) shows the changes of f_g and f_l during the grip-force control for $\mu = 0.3$. In the figure, the solid line denotes f_g and the dotted line denotes f_l. The change of estimated Φ using the eccentricity is shown by the solid line in Fig. 8(b). In the figure, the dashed line denotes Φ_d. As observed in the figure, Φ increases when f_l increases, however Φ is converged smoothly and rapidly to the target value by the grip force control. As a result, a grasp with desired slip margin can be maintained without occurring the gross slip. Similarly, the result $\mu = 0.8$ is shown Fig. 9. In these experiments, the same feedback parameter used in $\mu = 0.3$ is applied. The grip-force control sufficiently adapted to the change of the friction coefficient.

VI. Conclusion

In this paper, a grip-force control of an elastic object based on a visual slip margin feedback has been presented. The slip margin is estimated based on the analysis of the Hertzian contact. The slip margin is estimated in high-resolution by using the eccentricity rather than by the direct measurement of the displacement from the captured image. The experimental results have shown that the grip force is controlled without knowing the friction coefficient. The proposed method has been applied to a robotic gripper with transparent and rigid fingertip for grasping an elastic object in this paper; however, the estimating method of the slip margin itself can be applied to a soft and transparent fingertip for grasping a rigid object.

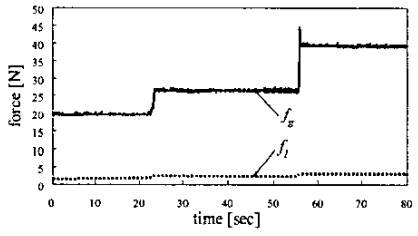

(a) Grip Force(f_g) and Load Force(f_l)

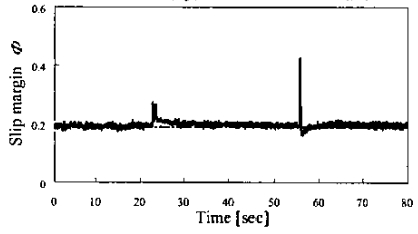

(b) Estimated Slip Margin (Φ)

Fig. 8. Experimental Result ($\mu = 0.3$)

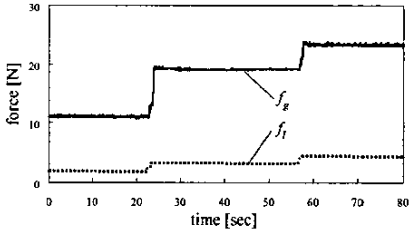

(a) Grip Force(f_g) and Load Force(f_l)

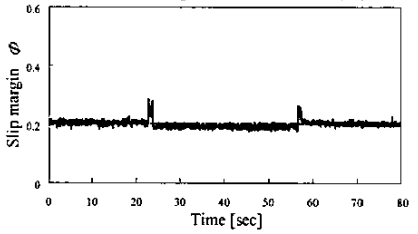

(b) Estimated Slip Margin (Φ)

Fig. 9. Experimental Result ($\mu = 0.8$)

References

[1] R. S. Johansson and G. Westling, "Roles of glabrous skin receptors and sensorimotor memory in automatic control of precision grip when lifting rougher or more slippery objects", *Exp. Brain Res.*, Vol.56, pp.550–564, 1987.

[2] N. J. Ferrier, R. W. Brockett, "Reconstructing the Shape of a Deformable Membrane using Image Data", *Int. J. Robotics Research*, Vol. 19, No. 9, pp. 795–816, 2000.

[3] M.R. Tremblay and M.R. Cutkosky, "Estimating Friction Using Incipient Slip Sensing During a Manipulation Task", *Proc.IEEE Int. Conf. Robotics and Automation*, pp. 363–368, 1993.

[4] H. Shinoda and S. Ando, "Ultrasonic Emission Tactile Sensor for Contact Localization and Characterization", *Proc. IEEE Int. Conf. Robotics and Automation*, Vol.3, pp.2536–2543, 1994.

[5] T. Maeno, T. Kawai and K. Kobayashi, "Analysis and Design of a Tactile Sensor Detecting Strain Distribution inside an Elastic Finger, *Proc. IEEE/RSJ Int. Conf. Intelligent Robots and Systems*Cpp. 1658–1663, 1998.

[6] C. Melchiorri, "Slip detection and control using tactile and force sensors", *IEEE Trans. on Mechatronics*, Vol.5, No.3, pp.235–243, 2000.

[7] T. Maeno, S. Hiromitsu and T. Kawai, " Control of Grasping Force by Detecting Stick/Slip Distribution at the Curved Surface of Elastic Finger", *Proc. IEEE Int. Conf. Robotics and Automation* Cpp. 3896–3901, 2000.

[8] H. Hertz, *On the contact of rigid elastic solids and on hardness*, English translation, Macmillan, 1896.

[9] Y. Kurita, A. Ikeda, J. Ueda, Y. Matsumoto and T. Ogasawara, "A Novel Pointing Device Utilizing the Deformation of the Fingertip", *Proc. IEEE/RSJ Int. Conf. Intelligent Robots and Systems*, pp.13–18, 2003.

[10] R.D. Mindlin, "Compliance of elastic bodies in contact", *Trans. ASME, J. Applied Mech.*, Vol.16 of *E*, pp.259–268, 1949.

[11] N. Xydas and I. Kao, "Modeling of Contact Mechanics and Friction Limit Surface for Soft Fingers in Robotics with Experimental Results", *Int. J. Robotics Research*, Vol. 18, No. 8, pp.941–950, 1999.

[12] M. Tada, T. Shibata, and T. Ogasawara, "Investigation of the touch processing model in human grasping based on the stick ratio within a fingertip contact interface", *Proc. IEEE Int. Conf. Systems, Man and Cybernetics*, tp1n4, 2002.

[13] R. M. Corless, G. H. Gonnet, D. E. G. Hare, D. M. Jeffrey, D. E. Knuth, "On the Lambert W Function", *Advances in Computational Mathematics*, Vol. 5 , pp. 329–359, 1996.